*Monografías del Semin. Matem. García de Galdeano.* **27:** 145–152, (2003).

# Upwind numerical techniques applied to the simulation of dam break flows

P. Brufau and P. García-Navarro

Fluid Mechanics Group

Centro Politécnico Superior

Universidad de Zaragoza

**Abstract**

An ideal scheme for the solution of multidimensional non-linear systems of partial differential equations governing fluid motion has not been found yet despite years of research effort and many scientific contributions. In the context of finite volume approximations based on flow dependent schemes, discussion is opened as to whether upwind or multidimensional upwind schemes are preferable for solving 2D problems. In this work we consider the use of upwind and multidimensional upwinding techniques for 2D shallow water flows, in particular, to the simulation of dam break flows. The basis of the two numerical methods is stated and the particular adaptation to the shallow water system is described. As test cases, laboratory experimental data supplied by partners of the Working Group on Dam Break Flow Modelling (CADAM) are used.

**Keywords**: upwind methods, dam break flow, finite volumes

**AMS Classification**: 75F2359

## 1 Introduction

Upwind schemes [1, 2, 9, 11] are accepted as accurate methods for the numerical solution of systems of conservation laws in one dimension. Attempts of applying these techniques in higher dimensions have generally relied on essentially one-dimensional algorithms combined with some form of operator splitting. Indeed, the standard extension of the finite volume methods is still to solve one-dimensional Riemann problems created at the interfaces of the finite volumes by the discontinuities in the reconstruction stage of the algorithm. When extended in this way many features of the flow, particularly if they are not aligned with the grid, can be completely misinterpreted by the numerical scheme.

A class of upwind methods has emerged which attempts to model the equations in a genuinely multidimensional manner [1, 3, 4, 5, 6, 7]. These schemes are designed to

monitor the average time evolution of the approximation to the solution within a complete grid cell rather than concentrating on the activity at the interfaces. Multidimensional upwind schemes were developed initially for the approximation of steady state solutions of the two-dimensional Euler equations on unstructured triangular grids, although they could be applicable to any system of hyperbolic conservation laws. One such case is given by the shallow water equations [4, 5].

Here, the performance of an upwind and a multidimensional upwind technique for 2D shallow water flows is described in first order accuracy. In the next sections, the basis of the numerical methods is stated and the application to the simulation of 2D dam break flows is presented.

# 2 Governing equations

Depth averaging of the free surface flow equations under the shallow water hypothesis leads to a common version of the 2D shallow water equations which, in conservative form is,

$$\frac{\partial \mathbf{U}}{\partial t} + \nabla \cdot (\mathbf{F}, \mathbf{G}) = \mathbf{H} \tag{1}$$

with

$$\mathbf{U} = \begin{pmatrix} h \\ hu \\ hv \end{pmatrix} \ , \ \mathbf{F} = \begin{pmatrix} hu \\ hu^2 + g\frac{h^2}{2} \\ huv \end{pmatrix} \ , \ \mathbf{G} = \begin{pmatrix} hv \\ huv \\ hv^2 + g\frac{h^2}{2} \end{pmatrix},$$

$$\mathbf{H} = \begin{pmatrix} 0 \\ gh\left(S_{0x} - S_{fx}\right) \\ gh\left(S_{0y} - S_{fy}\right) \end{pmatrix} \tag{2}$$

where $\mathbf{U}$ represents the vector of conserved variables ($h$ depth of water, $hu$ and $hv$ unit discharges along the coordinate directions), $\mathbf{F}$ and $\mathbf{G}$ are the fluxes of the conserved variables across the edges of a control volume. They consist of the convective fluxes together with the hydrostatic pressure gradients. $\mathbf{H}$ is the source term.

In addition, $u$ and $v$ are the velocities in the $x$, $y$ directions respectively, $g$ is the acceleration due to the gravity, $S_{0x}$, $S_{0y}$ are the bed slopes and $S_{fx}$, $S_{fy}$ the friction terms in the $x$, $y$ directions. For the friction term, the Manning equation has been used.

# 3 Numerical models

## 3.1 Upwind method

A cell centered finite volume method is formulated for equation (1) over a triangular control volume where the dependent variables of the system are represented as piecewise constants. The integral form of (1) for a fixed area $S$ is

$$\int_S \frac{\partial \mathbf{U}}{\partial t} dS + \int_S \nabla \cdot (\mathbf{F}, \mathbf{G})\, dS = \int_S \mathbf{H} dS \tag{3}$$

and, applying the divergence theorem to the second integral, we obtain

$$\int_S \frac{\partial \mathbf{U}}{\partial t} dS + \oint_C (\mathbf{F}, \mathbf{G}) \cdot \mathbf{n} dC = \int_S \mathbf{H} dS \tag{4}$$

where $C$ is the boundary of the area $S$, and $\mathbf{n}$ is the outward unitary normal vector. Given a computational mesh defined by the cells (volumes) of area $S_i$, where $i$ is the index associated with the centroid of the cell in which the cellwise constant values of $\mathbf{U}$ are stored, equation (4) can be represented by

$$\frac{d\mathbf{U}_i}{dt} S_i + \oint_{C_i} (\mathbf{F}, \mathbf{G}) \cdot \mathbf{n} dC = \mathbf{H}_i S_i \tag{5}$$

where a mesh fixed in time is assumed. The contour integral is approached via a mid-point rule, i.e., a numerical flux is defined at the mid-point of each edge, giving

$$\oint_{C_i} (\mathbf{F}, \mathbf{G}) \cdot \mathbf{n} dC \approx \sum_{k=1}^{NE} (\mathbf{F}, \mathbf{G})^*_{w_k} \cdot \mathbf{n}_{w_k} dC_{w_k} \tag{6}$$

where $w_k$ represents the index of edge $k$ of the cell, $NE$ is the total number of edges in the cell. The vector $\mathbf{n}_{w_k}$ is the unit outward normal, $dC_{w_k}$ is the length of the side, and $(\mathbf{F}, \mathbf{G})^*_{w_k}$ is the numerical flux tensor.

The evaluation of the numerical flux in equation (6) is based on the Riemann problem defined by the conditions on the left and right sides of the cell edges. An important feature of the 1D upwind schemes for non-linear systems of equations is exploited here. This is the definition of the approximated flux jacobian, $\tilde{A}_{i+\frac{1}{2}}$, constructed at the edges of the cells and satisfying special conditions [9]. The 2D numerical upwind flux in equation (6) is obtained by applying the expression of the numerical flux across the interface $i + \frac{1}{2}$ of a cell in a 1D domain to each edge $w_k$ of the computational cell in a 1D form. The 1D philosophy is followed along the normal direction to the cell walls, making use of the normal numerical fluxes leading to an ordinary differential equation that can be integrated by standard methods such as a forward Euler time integration procedure.

$$\mathbf{U}_i^{n+1} = \mathbf{U}_i^n - \frac{\Delta t}{S_i} \left( \sum_{k=1}^{NE} (\mathbf{F}, \mathbf{G})^*_{w_k} \cdot \mathbf{n}_{w_k} dC_{w_k} \right)_i^n + \Delta t \mathbf{H}_i^n \tag{7}$$

## 3.2 Multidimensional upwind method

The application of this technique to the shallow water system requires that the equations are written in terms of the conserved variables, so that (1) can be expressed in its non-conservative form as

$$\frac{\partial \mathbf{U}}{\partial t} + \frac{\partial \mathbf{F}}{\partial x} + \frac{\partial \mathbf{G}}{\partial y} = 0 \tag{8}$$

in which only the homogeneous part has been considered. It is useful to express the equations in terms of the primitive variables

$$\mathbf{V} = (h, u, v)^T \tag{9}$$

in a non-conservative way, as

$$\frac{\partial \mathbf{V}}{\partial t} + R\frac{\partial \mathbf{V}}{\partial x} + S\frac{\partial \mathbf{V}}{\partial y} = 0 \tag{10}$$

In the conservative formulation, the fluctuation is defined as

$$\phi_T = \int_T \mathbf{U}_t dS = -\int_T (\mathbf{F}_x + \mathbf{G}_y) dS \tag{11}$$

We can use the relation between the two sets of variables to define new matrices $R$ and $S$,

$$\begin{aligned} R &= \frac{\partial \mathbf{F}}{\partial \mathbf{V}} = \frac{\partial \mathbf{F}}{\partial \mathbf{U}}\frac{\partial \mathbf{U}}{\partial \mathbf{V}} = AM \\ S &= \frac{\partial \mathbf{G}}{\partial \mathbf{V}} = \frac{\partial \mathbf{G}}{\partial \mathbf{U}}\frac{\partial \mathbf{U}}{\partial \mathbf{V}} = BM \end{aligned} \tag{12}$$

so that

$$\mathbf{F}_x + \mathbf{G}_y = R\mathbf{V}_x + S\mathbf{V}_y \tag{13}$$

Provided that the variables $\mathbf{V}$ are linear over the cells $T$, the gradients, $\mathbf{V}_x$ and $\mathbf{V}_y$, are constant, and we can write the fluctuation as

$$\phi_T = -S_T[\bar{R}\mathbf{V}_x + \bar{S}\mathbf{V}_y] \tag{14}$$

with the definitions:

$$\bar{R} = \frac{1}{S_T}\int_T R(\mathbf{V})dS, \quad \bar{S} = \frac{1}{S_T}\int_T S(\mathbf{V})dS \tag{15}$$

We approximate $\bar{R}$, $\bar{S}$ by

$$\bar{R} \approx R(\bar{\mathbf{V}}), \qquad \bar{S} \approx S(\bar{\mathbf{V}}) \tag{16}$$

where the averaged variables are simply

$$\bar{\mathbf{V}} = \begin{pmatrix} \bar{h} \\ \bar{u} \\ \bar{v} \end{pmatrix} = \frac{1}{3} \begin{pmatrix} h_1 + h_2 + h_3 \\ u_1 + u_2 + u_3 \\ v_1 + v_2 + v_3 \end{pmatrix} \tag{17}$$

summing over the nodal values at the vertices of the triangle $T$. Note that with this definition of $\bar{R}$, $\bar{S}$ we are only approximating equation (11). As a consequence, we lose conservation in the numerical evaluation of the fluctuation.

The next step consists on computing the fluctuations and distributing them [8] to the vertices of every cell by means of an advection scheme [3]. This last step requires the description of wave models [10] and the choice of an advection scheme.

# 4 Numerical results

Results obtained with first order upwind and multidimensional upwind approximations on unstructured Delaunay triangular meshes for the experimental test case proposed by Prof. Zech (Civil Engineering Dpt., UCL Belgium) from the Working Group on Dam Break Flow Modelling are going to be presented. The test combines a square shaped upstream reservoir and a $45^o$ bend channel (see Fig. 1). The flow will be essentially two-dimensional in the reservoir and at the angle between the two straight reaches of the $45^o$ bend channel. Two features of the dam break resulting flow are of special interest: the damping effect of the corner, and the upstream moving hydraulic jump which is formed by reflection at the corner.

The initial conditions are water at rest with the free surface $25cm$ in the upstream reservoir and $1cm$ water depth in the channel. All boundaries are solid non-slip walls except the outlet which is considered free. The Manning coefficient is $n_b = 0.0095$ for the bed. The number of elements used in the mesh is 15397. Nine gauging points were used in the laboratory to measure water level in time. Their location is shown in Fig. 1. The measurements at these stations are compared to the numerical results and displayed in Fig. 2. In Fig. 3 the free surface is described at time $10s$.

In general, the figures indicate a good performance of the two numerical schemes. The arrival times of the main shock fronts is better captured by the upwind method. Some differences are noticeable in P3 and P4 as the reflected shock front celerity is concerned. This may be attributed to the treatment of the boundary conditions. The great difference between the results obtained with both schemes is referred to the free surface plot. Perhaps

measurements along the walls of the channel should be taken into account to demonstrate which approximation is better. Till now, only data in the central axis have been measured.

# 5 Conclusions

An upwind and a multidimensional upwind scheme for the solution of the 2D shallow water equations has been applied in first order accuracy for dam break modelling. The numerical results have been validated by comparison with experimental data in one test case. Differences on the results obtained with both techniques do not follow a clear tendency and it is difficult to establish the superiority of one over another. In the test case presented, both results fail to reproduce exactly the arrival times of the reflected wave (P2 and P3 gauge points). This suggests that the reflection at the corner may require an improved numerical treatment. Moreover, differences can be noticed at the free surface plots. Reflected waves from the walls are clearly observed in the multidimensional upwind results and perhaps a good test could be performed taking measures along the channel walls to give a new point of view in the numerical analysis.

# 6 Bibliography

# References


[1] Brufau P., *Simulación bidimensional de flujos hidrodinámicos transitorios en geometrías irregulares*. PhD Thesis, University of Zaragoza, Spain (2000).

[2] Brufau P. and García-Navarro P., Two dimensional dam break flows in unstructured grids, *Hydroinformatics98*, Copenhague, Denmark (1998).

[3] Deconinck H., Struijs R., Bourgois G., Paillere H. and Roe P.L., Multidimensional Upwind Methods for Unstructured Grids, *Unst. Grid Met. for Advec. Domin. Flows, AGARD, 787* (1992).

[4] García-Navarro P., Hubbard M.E. and Priestley A., Genuinely Multidimensional Upwinding for the 2D Shallow Water Equations, *J. Comp. Phys., 121*, pp. 79-93 (1995).

[5] García-Navarro P., Hubbard M.E. and Brufau P., *Godunov Methods: Theory and Applications. Multidimensional upwind schemes: application to hydraulics*. Kluwer Ac. Press (2000).

[6] Hubbard M.E., Multidimensional Upwinding and Grid Adaptation for Conservation Laws, PhD Thesis, University of Reading, England (1996).

[7] Hubbard M.E. and Baines M.J., Conservative multidimensional upwinding for the steady two dimensional shallow water equations. *J. Comp. Phys.*, **vol. 138**, pp. 419-448 (1997).

[8] Paillere H., Multidimensional Upwind Residual Distribution Schemes for the Euler and Navier-Stokes Equations on Unstructured Grids, PhD Thesis, University of Brussels, Belgium (1995).

[9] Roe P.L., A Basis for Upwind Differencing of the Two-Dimensional Unsteady Euler Equations, *Num. Met. Fluid Dyn. II* (1986).

[10] Rudgyard M., Multidimensional Wave Decompositions for the Euler Equations, *VKI Lecture Series, Comput. Fluid Dynam.* (1993).

[11] Sleigh P.A., Berzins M., Gaskell P.H. and Wright N.G., An Unstructured Finite Volume Algorithm for predicting flow in rivers and estuaries, *Comp. and Fluids* (1997).

# 7 Figures

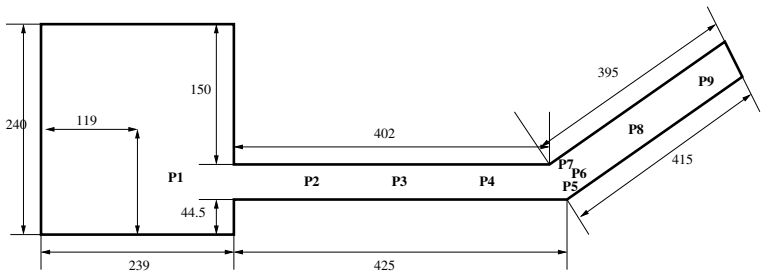


Figure 1: Plane view of the channel.

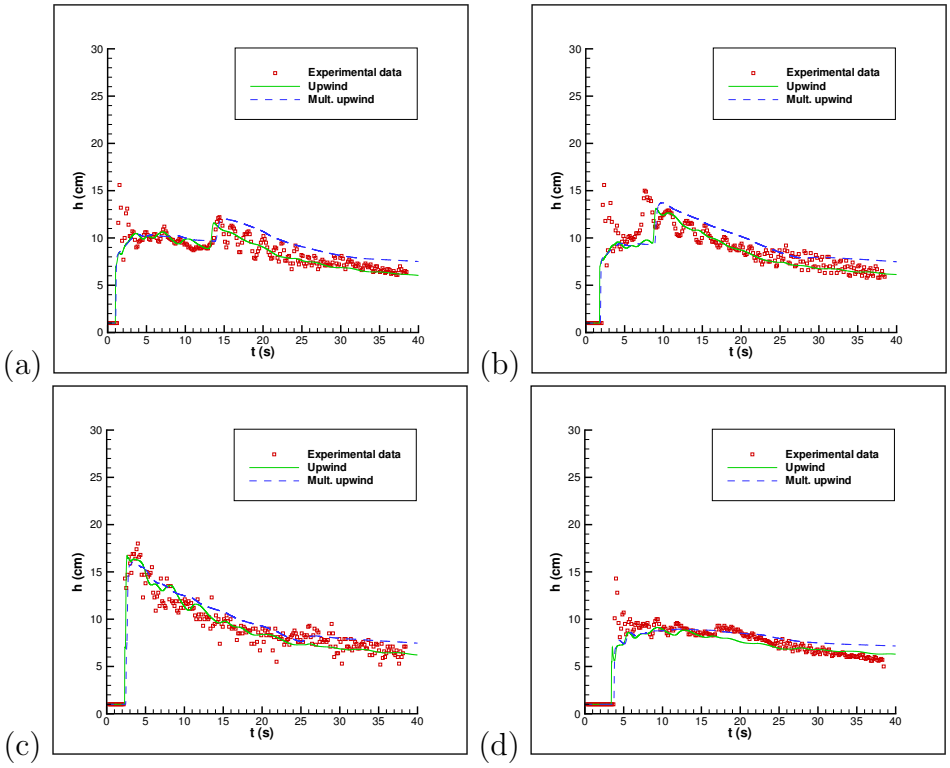


Figure 2: Water depth history at points a) P3, b) P4, c) P5 and d) P9.

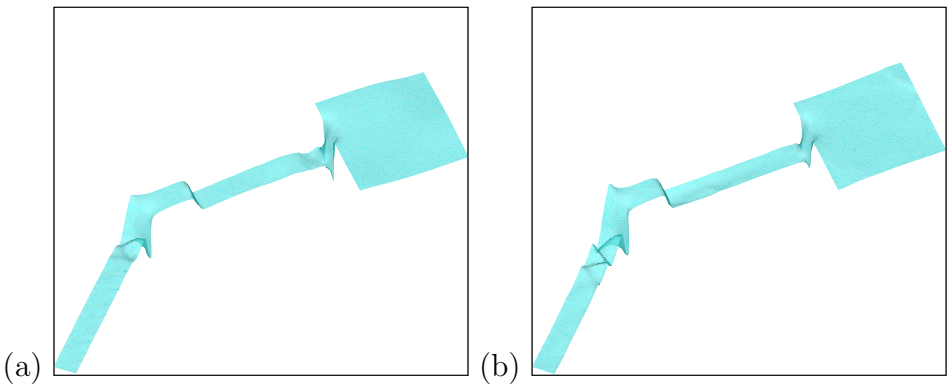


Figure 3: Free surface at time t=10s with upwind (a) and multidimensional upwind schemes (b).